ELSEVIER

Journal of Alloys and Compounds 323–324 (2001) 107–110

Journal of ALLOYS AND COMPOUNDS

www.elsevier.com/locate/jallcom

Gd thin films: relationship between elastic properties and microstructure

J. Rubio-Zuazo*, M. Vila, A. Muñoz-Martín, A. de Bernabé, C. Prieto

Instituto de Ciencia de Materiales de Madrid, Consejo Superior de Investigaciones Científicas, Cantoblanco, 28049 Madrid, Spain

Abstract

A set of gadolinium thin films was prepared over Si(100) substrates by DC-operated planar magnetron sputtering deposition. This paper reports a change in the film texture by changing the sputtering working Ar gas pressure. An X-ray study of their structural properties shows that films have (0002) and (1010) orientations. On the other hand, their elastic properties have been studied by Surface Brillouin Light Scattering spectroscopy that provides the velocity of the surface acoustic waves. A simulation that takes into account values of thin film density and elastic constants tensor identical to the corresponding for bulk gadolinium shows good agreement between theory and experiment for (0002)-textured samples. Nevertheless, (1010)-textured films seem to have slightly different values of the elastic constant.

Keywords: Thin films; Vapour deposition; X-ray diffraction; Elasticity; Inelastic light scattering

1. Introduction

The extremely high neutron absorption cross section of natural mixture of gadolinium isotopes let neutrons be absorbed in such a thin layer that the conversion electrons from the low lying transitions of the gamma cascade can escape easily and can be detected in a thin semiconductor surface detector [1,2]. Typical Gd film thickness is about 10 μm for natural gadolinium converter but it can be reduced one or two orders of magnitude by preparing a ^{157}Gd isotope thin film.

Within this scenario, it is very important to characterize the microstructural and mechanical properties of Gd thin films. We present the study of crystallinity and texture properties of Gd thin films grown on Si(100) wafers by DC magnetron sputtering. In order to relate film characteristics with the mechanical properties, their elastic properties have been measured by Surface Brillouin Light Scattering (SBLS) spectroscopy. This method consists in detecting the Surface Acoustic Waves (SAW) and the guided modes by the inelastic scattering of light by the acoustic phonons [3]. In thin films, Brillouin spectroscopy permits the obtention of the phase velocity for SAW and guided modes (Rayleigh and Sezawa modes) that are related with the elastic constants of the thin film and the substrate materials [4].

In this work, we show that in order to explain the elastic behavior of the Gd thin films, the microstructural characterization should be taken into account. In particular, one of the most interesting and important aspects when measuring elastic properties in thin films is the study of the film texture. A change in the material orientation may be accompanied of a variation of the elastic properties. Gd is a typical hexagonal metal with *hcp* structure that complicates the analysis of the elastic properties because of the particular symmetry and because of the five independent terms in the elastic constants tensor.

2. Experimental

Gadolinium thin films were grown on naturally oxidized Si(100) substrates at room temperature using a 2-in planar magnetron source (Angstrom Science). The sputtering system is equipped with a Huttinger DC-power supply. The vacuum system provides a residual pressure in the range of 10^{-7} mbar. Working Ar pressure for sputtering deposition was in the 10^{-3} mbar. The applied power to magnetron cathode was about 4 W. After growing, all samples were exposed to the air and immediately X-ray diffraction and SBLS experiments were performed.

X-ray diffraction (XRD) experiments were performed on Bragg–Brentano geometry in order to test the texture of the samples. Film thickness was determined from the Kiessig fringes of specular X-ray reflectivity (XRR) patterns [5]. Both experiments were performed on a standard two-circle diffractometer Siemens D-500.

*Corresponding author.

0925-8388/01/$ – see front matter
PII: S0925-8388(01)00984-7

In order to know deposition rate, two types of measurements have been performed: film thickness has been monitored 'in-situ' by a quartz balance and some samples have been selected for calibration purposes and their thickness have been measured by XRR. Fig. 1(a) shows the XRR data of a 29-nm thick sample; multiple oscillations guarantee the high flatness of the samples. Fig. 1(b) presents the deposition rate as a function of the working Ar pressure. That rate shows a usual behavior having a maximum near 7×10^{-2} mbar. Within this range of pressures, it can not be observed some insight of any anomaly in the rate deposition.

SBLS spectroscopy experimental set-up can be described as follows: The monochromatic source of light used was a 2060 Beamlok Spectra Physics Ar-ion laser with a wavelength of 514.5 nm. It is provided with an intracavity temperature stabilized single mode and single-frequency *z*-lok etalon. The scattered light is analyzed using a JRS tandem Sandercock-type 3+3 pass [6]. The incident polarization direction was chosen to be in plane (*P* polarization) while no polarization analysis of the scattered light was made. The free spectral range chosen was 20 GHz and the usual backscattering geometry was used [7]. Even if no vertical slit was placed at the focusing-collecting lens, its dimensions were chosen to minimize the wavevector dispersion. In order to avoid photomultiplier damage, the elastic peak was filtered using a JRS Scanning-synchronized reference beam system.

3. Results and discussion

We have observed that samples are highly textured in different directions depending on the deposition gas pressure. Samples prepared with Ar gas pressure smaller than 3×10^{-3} mbar are highly textured in the (1010) direction, and in the (0002) for samples prepared with Ar gas pressure larger than 5×10^{-3} mbar. Fig. 2 shows XRD data of two samples prepared at Ar pressures of 5×10^{-3} and 3×10^{-3} mbar and with very similar thickness (414 and 397 nm, respectively). They show 99% texturation degree in the (0002) direction and 98% texturation degree in the (1010) direction.

Fig. 3 shows typical Brillouin spectra of these samples. The experimental peaks have been fitted with Gaussians in order to determine their positions respect to the elastic laser line. The Brillouin shifts are converted to sound velocities by $V^{SAW} = \nu_B/(2\ k_i \sin\theta)$. V^{SAW} is the surface acoustic wave velocity, ν_B is the Brillouin shift, θ_i is the angle between the incident light and the normal to the surface and k_i is the incident light wavevector. The peak with the smallest Brillouin shift is the Rayleigh mode corresponding to the phonon propagating in the surface. Peaks of higher Brillouin shifts correspond to Sezawa modes [4–6]. These modes are bulk transverse modes with an additional longitudinal component localized at the

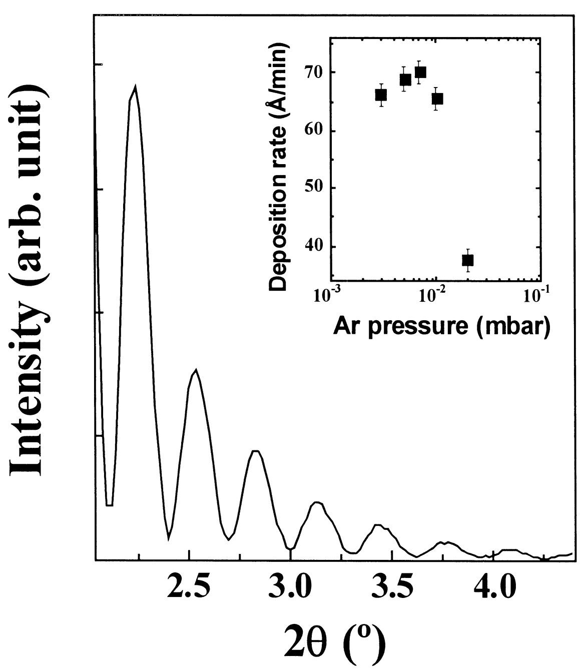

Fig. 1. Low angle X-ray reflectivity spectra showing the Kiessig fringes to determine the film thickness (see text). The inset shows the dependence of the deposition rate with the sputtering Ar pressure.

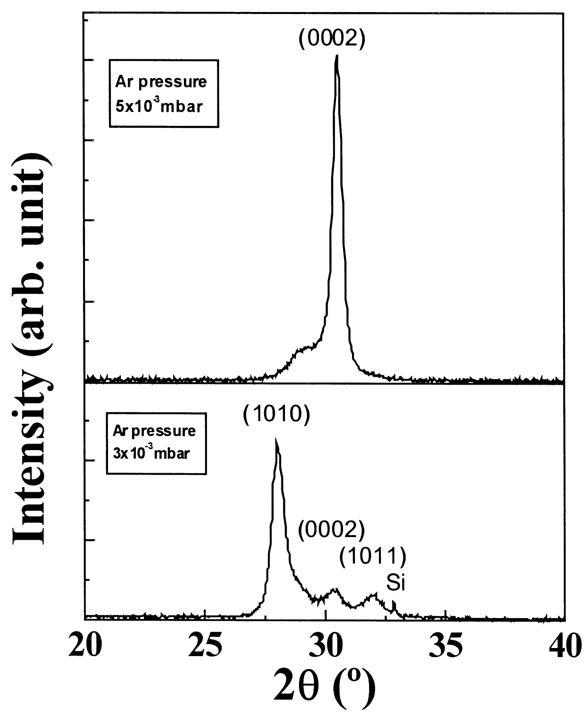

Fig. 2. High angle X-ray diffraction of two Gd thin films, of approximately 400 nm thick, showing the two different textures. (a) Sample prepared at 5×10^{-3} mbar Ar pressure. (b) Sample prepared at 3×10^{-3} mbar.

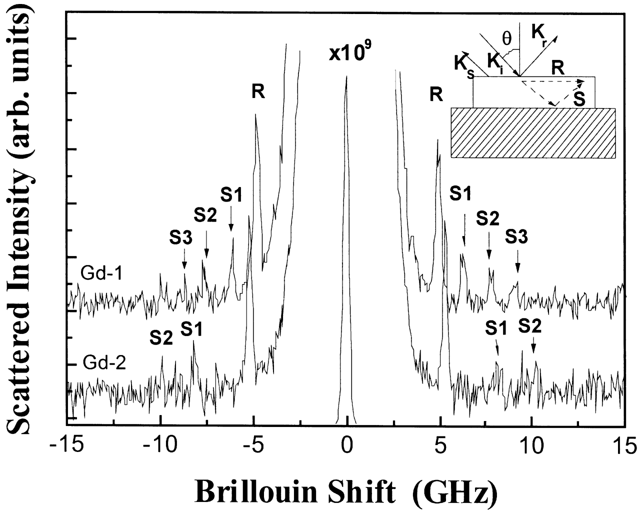

Fig. 3. Surface Brillouin Light scattering spectra of two Gd films, the incident angle was $\theta_i = 60°$. Gd-1 and Gd-2 samples have thickness of 414 and 198 nm and were prepared with Ar pressure of 5×10^{-3} and 3×10^{-3} mbar, respectively. R and S denotes Rayleigh and Sezawa modes, respectively.

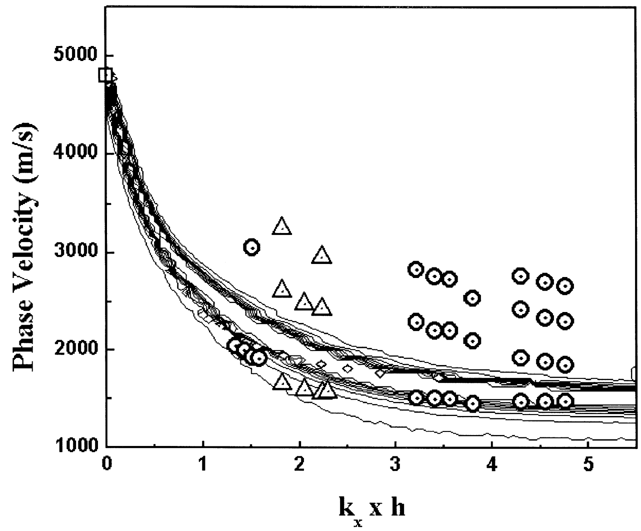

Fig. 4. Contour Brillouin intensity as a function of the surface wave phase velocity and $k_x \times h$ for Gd films over Si(100). Circles and squares represent experimental points and lines and contours are calculations based on effective elastic constants of the system. Circles and triangles are data from samples textured in the (0002) and (1010) crystallographic planes of symmetry, respectively.

surface, they correspond to waves trapped in the interface film-substrate propagating parallel to the surface along the interface due to total internal reflection (see inset in Fig. 3). These modes only appear when the transverse velocity in the substrate is higher than the transverse velocity in the film and are dependent on the crystal orientation, so they should be dependent of the surface texture.

The influence of the substrate on the elastic properties of a deposited layer play an important role that can be measured in an experiment showing the dependence of the sound velocity as a function of the adimensional parameter $k_x \times h$, where k_x is the projection over the surface of the incident wavevector and h is the film thickness. Obviously, this adimensional parameter can be varied by changing the sample thickness and by performing a sagital dispersion varying the incident angle. Such kind of representation is shown on Fig. 4 where the lowest velocity branch corresponds to the Rayleigh mode. For $k_x \times h$ equal to zero, the velocity measured is the corresponding to the substrate, while when $k_x \times h$ is very large, due to the increment of the film thickness, the velocity measured is the corresponding to the film free from the substrate. For intermediate $k_x \times h$ values, the obtained velocity is a mixture of substrate and film. In our case velocities decrease because the substrate is harder than the film. Beyond a $k_x \times h$ value, Rayleigh mode velocity becomes independent of the thickness, meaning that the film is not influenced by the substrate and the so-called 'sinus law' is followed by the Rayleigh peak. Sezawa modes appear at a critical thickness and obey the similar law as the Rayleigh mode.

A simulation program was used to fit the dependence of the sound velocity [8]. This simulation program calculates the Brillouin spectrum of an opaque layer over a substrate. It takes into account the light scattering by the ripple mechanism and is based on the effective elastic constant of the films/substrate system, details have been given elsewhere [8,9]. Fits can be done by a trial-and-error method. Once a good fit had been obtained the effective elastic constants of the film were varied arbitrarily up to a clear separation of calculated branches from the experimental points (see Fig. 4), this variation is taken as the error bar (which turned out to be less than 1 GPa). The calculations corresponds to three-dimensional graphs whose usual representation is a contour plot. In this type of plots, the maxima (which represent the Brillouin peaks) correspond to zones with high density of lines, as well as white regions between these zones with high density of lines. In principle, Rayleigh or Sezawa modes can be simulated, but in this Gd/Si(100) system we have focussed our attention only in the Rayleigh branch.

Experimental data (circles and triangles) of the surface and bulk acoustic wave velocity are given in Fig. 4 as a function of the adimensional magnitude $k_x \times h$. They have been obtained for several samples and several incident angles. The velocity dispersion shows a typical behavior, which is approximately followed by all the samples. Nevertheless, a small difference may be observed for (1010)-textured samples respect to the (0002)-textured ones. The simulation of the phase velocity dispersion for the system formed by a Si(100) substrate and a Gd film is given in Fig. 4. In order to perform this simulation, we have taken the gadolinium bulk density ($\rho = 7.9$ g/cm^3) and the bulk gadolinium reported C_{ij} data ($C_{11} = 67.8$ GPa, $C_{33} = 71.2$ GPa, $C_{44} = 20.8$ GPa, $C_{12} = 25.6$ GPa and $C_{13} = 20.7$ GPa) [10]. The experimentally determined velocity dispersion for (0002)-textured thin film samples is very well reproduced by the simulation, it allows to conclude that values of both magnitudes (density and elastic constants tensor) of thin films are identical to those corresponding to bulk gadolinium. On the other hand, (1010)-textured thin films (triangles in Fig. 4) seem to have different C_{ij} values, but in order to verify that observation it will be necessary to perform a detailed study on a set of samples with the adequate thickness range to fit the whole velocity dispersion curve.

4. Conclusions

It has been proved that highly textured Gd thin films can be obtained, at least with two different orientations, by changing the sputtering pressure (Ar). The elastic characterization carried out by Surface Brillouin Light Scattering spectroscopy in (0002)-textured Gadolinium thin films supply data of the elastic constants of the films/substrate system that can be explained in terms of the bulk gadolinium and silicon elastic constants. The phase velocity of surface acoustic waves seems to have a small dependence on the texture of the thin films.

Acknowledgements

This work has been partially supported by CICyT under grant numbers MAT97-0725 and 1FD97-1305.

References

[1] M.W. Johnson, in: H. Morsi, N. Kroó, C. Ayache (Eds.), Progress in Detector, European Communities, Luxembourg, 1998, p. 61.
[2] H. Rauch, in: H. Morsi, N. Kroó, C. Ayache (Eds.), Progress in Detector, European Comunities, Luxembourg, 1998, p. 64.
[3] M. Grimsditch, in: M. Cardona, G. Güntherodt (Eds.), Light Scattering in Solids V, Springer-Verlag, Berlin, 1989.
[4] C. Prieto, A. de Bernabé, R. Castañer, A. Muñoz-Martín, R.J. Jiménez-Rioboó, M. García-Hernández, A. de Andrés, J. Phys. Condens. Matter. 12 (2000) 2931–2943.
[5] A. de Bernabé, M.J. Capitán, H.E. Fischer, C. Prieto, J. Appl. Phys. 84 (1998) 1881.
[6] J.R. Sandercock, in: M. Cardona, G. Güntherdot (Eds.), Light Scattering in Solids III, Springer-Verlag, Berlin, 1982.
[7] P. Mutti, C.E. Bottani, G. Ghislottie, M. Beghi, G.A.D. Briggs, J.R. Sandercock, in: G.A.D. Briggs (Ed.), Advances in Acoustic Microscopy, Vol. 1, Plenum, New York, 1995.
[8] X. Zhang, J.D. Comins, A.G. Every, P.R. Stoddart, W. Pang, T.E. Derry, Phys. Rev. B 58 (1998) 13677.
[9] A. Marvin, V. Bortolani, F. Nizzoli, G. Santoro, J. Phys. C 13 (1980) 1607.
[10] Landolt-Börstein, in: K.H. Hellwege (Ed.), Numerical Data and Function Relationships in Sciences and Technology, Vol. 11, Springer, Berlin, 1979.